Available online at www.sciencedirect.com
SCIENCE DIRECT®
European Journal of Medicinal Chemistry 41 (2006) 321–329
EUROPEAN JOURNAL OF MEDICINAL CHEMISTRY
http://france.elsevier.com/direct/ejmech

Original article

Adenosine receptor modelling. A_1/A_{2a} selectivity

Tiziano Tuccinardi, Gabriella Ortore, Clementina Manera, Giuseppe Saccomanni, Adriano Martinelli *

Dipartimento di Scienze Farmaceutiche, Università di Pisa, via Bonanno 6, 56126 Pisa, Italy

Received 8 February 2005; received in revised form 24 August 2005; accepted 28 September 2005
Available online 19 January 2006

Abstract

Three-dimensional models of the A_1 and A_{2a} adenosine receptors (AR) were constructed by means of a homology procedure, using bovine rhodopsin as a template. In order to validate the two models, a docking analysis of selective agonists was carried out. The study shows that A_1/A_{2a} selectivity is mainly influenced by the different ability of the two receptors to give lipophilic interactions, instead of giving different H bonds. The binding site cavity of the A_1AR is smaller than that of the A_{2a}AR, and for this reason, less bulky ligands like CPA are able to give close interactions with the A_1AR, unlike larger ligands such as CGS-21680. The different dimensions of the binding site cavity could be due to the presence of three residues of proline, which cause a different rearrangement of the TM, thus modifying the side chain disposition inside the inter-helix channel.

Keywords: Adenosine receptor; A_1; A_{2a}; Docking; Receptor modelling

1. Introduction

Adenosine receptors are members of the superfamily of G protein-coupled receptors (GPCR). As such, they are single polypeptide chains possessing seven hydrophobic transmembrane-spanning segments that couple to an effector molecule through a trimeric G protein complex.

To date, four adenosine receptor subtypes have been cloned; these include the A_1 and A_3 receptors, which inhibit adenylyl cyclase, and the A_{2a} and A_{2b} receptors, which stimulate adenylyl cyclase [1].

In the present study, we focused our attention on the interaction of ligands with the A_1 and A_{2a}ARs; the A_1AR was initially cloned from the thyroid gland of dogs [2], and was later isolated from several other species [3,4]. The A_1AR is a protein of 326 amino acids, which has a high affinity for N^6-substituted adenosine analogues. Several highly selective A_1AR compounds are available, including the agonist N^6-cyclopentyladenosine (CPA) [5]. The carboxyl terminus of the A_1AR is shorter than that of the A_{2a}AR, whereas the amino terminus is longer. At the amino acid level, the A_1 and A_{2a}ARs are generally 60% identical within the transmembrane domains [3,4,6]. Unlike the A_1AR, the A_{2a}AR has a high affinity for 5′-substituted adenosine agonists and a low affinity for N^6-substituted compounds [7]. Highly selective A_{2a}AR agonists are available, and include the compound CGS-21680 [8].

These receptors are important pharmacological targets in the treatment of a variety of conditions such as asthma, neurodegenerative disorders, psychosis and anxiety, chronic inflammatory diseases and many other physiopathological states that are believed to be associated with changes in adenosine levels [9–11].

In particular the development of agonists for the adenosine A_1AR receptor, able to mimic the central inhibitory effects of adenosine (and so inhibiting neurotransmitter release), may therefore be clinically useful as neuroprotective agents. On the contrary A_1AR selective antagonists have been developed as antihypertensives and potassium-saving diuretics, cognition enhancers and useful therapeutics for the alleviation of the symptoms of Alzheimer's disease [12,13].

Furthermore A_{2a}AR agonists are potentially useful for the treatment of cardiovascular diseases, such as hypertension, is-

* Corresponding author. Fax: +39 50 221 9605.
E-mail address: marti@farm.unipi.it (A. Martinelli).

0223-5234/$ - see front matter © 2006 Elsevier SAS. All rights reserved.
doi:10.1016/j.ejmech.2005.09.011

chemic cardiomyopathy, inflammation, and atherosclerosis [14,15], and A_{2a}AR antagonists have been proposed as novel therapeutics for Parkinson's disease and may also be active as cognition enhancers, neuroprotective and antiallergic agents, analgesics, and positive inotropics [16–18].

Consequently, selective and potent agonists or antagonists at the adenosine receptor subtypes are needed for therapeutic intervention; however, a clear picture of how these receptors bind their various ligands has not emerged yet.

Knowledge of the 3D structure of adenosine receptors could be of great help in the task of understanding their function and in the rational design of specific ligands. However since GPCRs are membrane-bound proteins, high-resolution structural characterisation is still an extremely difficult task.

For this reason, great importance has been placed on molecular modelling studies, and, in particular in the last few years, on homology modelling techniques. The publication of the first high-resolution crystal structure for rhodopsin [19], a GPCR superfamily member, provides the option of homology modelling to generate 3D models based on detailed structural information.

With the aim of achieving a better understanding of experimental results, in the present study we constructed the A_1AR and A_{2a}AR three-dimensional model of the seven α-helical transmembrane domains, using bovine rhodopsin as a template.

To test these models, we carried out the docking of certain A_1 and A_{2a}AR selective agonists.

2. Computational methods

All the calculations were carried out by means of the Batchmin programme of the MACROMODEL suite [20], using the Amber force field and making the dielectric "distance-dependent" constant equal to 4.0. The molecular dynamics (MD) simulations were performed at 300 K, with a time-step of 1.0 fs and an equilibration time of 40 ps, while all the minimisations were carried out by means of 2000 Steepest Descent steps, followed by Conjugate Gradient until a convergence of 0.05 kJ $mol^{-1}Å^{-1}$.

The graphic manipulations and visualisations were performed by means of the Maestro [20], WebLabViewer [21] and Chimera [22] programmes, while the quantum mechanical calculations were carried out using the Gaussian03 program [23].

2.1. Amino acid numbering

To refer to specific amino acids sequences, the numbering system suggested by Ballesteros and Weinstein [24] was used.

The most highly conserved residue in each transmembrane helix (TMH) was assigned a locant value of 0.50, and this number was preceded by the TMH number and followed in parentheses by the sequence number. The other residues in the helix were given a locant value relative to this.

2.2. Molecular modelling

All the information regarding the primary structure of human A_1 and A_{2a} receptors, and their subdivision into transmembrane, cytoplasmatic and extracellular domains, was obtained from the GPCR Data Bank [25]. We modelled only the TM domains, since the function of the loops has still not been defined. Although site-directed mutagenesis suggests a role for adenosine receptor loops, and in particular for the second extracellular (E2) ones, it remains unclear whether the E2 loop is in direct contact with ligands, or whether it contributes to the overall physical architecture of the receptor protein [26–28].

After defining the primary structure, the secondary and tertiary ones were defined by using the structure of bovine rhodopsin as a template [19].

The receptor–template superimposition was carried out maintaining the maximum analogy between the receptors, and choosing the regions with a conserved or semi-conserved sequence. The alignment was studied on several adenosine receptors by means of the ClustalW programme [29] using the blosum algorithm, with a gap open penalty of 10 and a gap extension penalty of 0.05.

As shown in Fig. 1, the alignment was guided by the highly conserved amino acid residues, including the D/ERY motif (D/E3.49, R3.50, and Y3.51), the two proline residues P4.50 and P6.50 and the NPXXY motif in TM7 (N7.49, P7.50, and Y7.53) [30].

We used the 3D X-ray crystallographic structure of bovine rhodopsin registered in PDB (1F88) as a direct template to construct the 7 TM helical structure of the A_1AR, using the Maestro programme to substitute the residues of rhodopsin not conserved in the receptor; subsequently, each model helix was capped with an acetyl group at the N-terminus and an *N*-methyl group at the C-terminus. In order to consider the mutagenesis data regarding TM3, it was necessary to rotate the third helix of the receptor by approximately 90°.

The A_1AR was subjected to a preliminary minimisation and 200 ps of MD, after which the final structure was minimised. When MD simulations are carried out in the gas phases, skipping the explicit environment requires the use of a set of restraints, to replace the natural stabilizing effects of the membrane bilayer on the TM domains. Accordingly, restraints with a force constant of 10 kcal mol^{-1} $Å^{-2}$ were applied to backbone for the first 100 ps, and for the remaining 100 ps, these restraints were reduced to 1 kcal mol^{-1} $Å^{-2}$.

The A_1AR model obtained by means of these calculations was complexed with a high-affinity ligand, and the complex was optimised.

CPA was chosen for this purpose, since it is commonly used in binding experiments as a radioligand [5]; it was docked into the receptor, bearing in mind the known mutagenesis data.

The CPA geometry was optimised at the AM1 level, and the atomic charges were calculated using the RESP [31] method with the 6-31G* wave function.

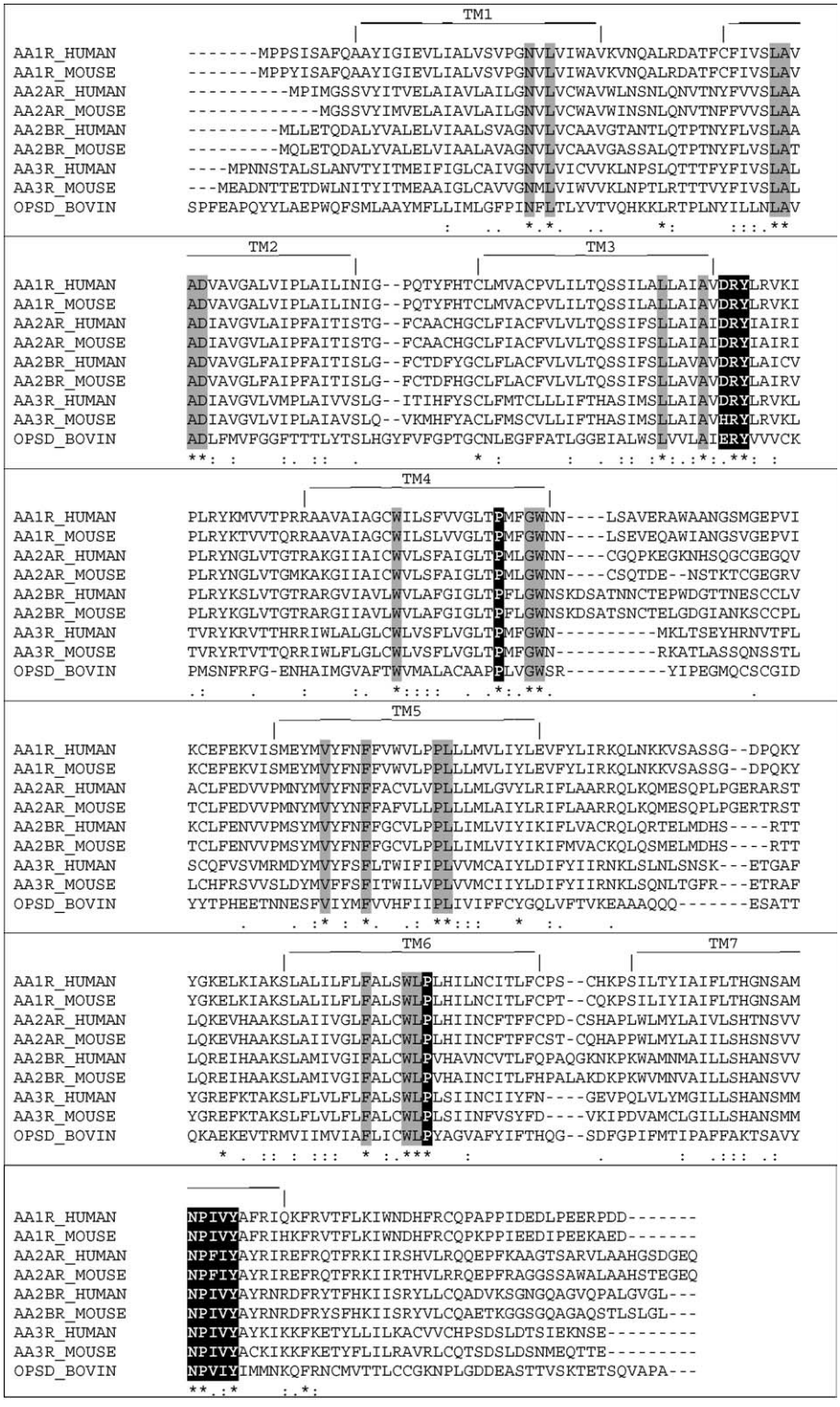

Fig. 1. Alignment of the adenosine receptors and bovine rhodopsin (OPSD_BOVIN) amino acid sequences. The highly conserved patterns of the D/ERY motif (D/E3.49, R3.50, and Y3.51), P4.50 and P6.50 and the NPXXY motif (N7.49, P7.50, and Y7.53) are marked with black. The other identical residues are indicated with "*" and marked in grey in the TMs, while the conservatively replaceable residues are indicated with ":" and ".".

The CPA was then manually introduced into the binding site in such a manner as to give H bond interactions with T3.36(91), S3.39(94), T7.42(277), and H7.43(278) and a lipophilic interaction (through the cyclopentyl moiety) with L3.33(88), in accordance with the main mutagenesis data (see Table 1).

The complex modelling was performed by means of a total of 800 ps of molecular dynamics. In order to consider the stabilizing presence of the membrane around the receptor, all the alpha carbons of the protein and the intra-helix H bonds were blocked during modelling by means of decreasing force con-

Table 1
Mutational analysis for A_1 and A_{2a}AR agonist interaction

	Gene Number	A_1AR	Mutational results	A_{2a}AR	Mutational results
TM1	1.37	G14	T: increased affinity [32]	T11	
	1.39	E16	A: reduced 4- to 40-fold [33]	E13	Q: slight reduction [34]
	1.48	P25	L: modest reduction [32]	L22	
	1.54	I31	C: no variation [32]	C28	
TM2	2.41	C46	A/S: no variation [35]	Y43	
	2.45	S50	A: no variation [32]	S47	
	2.50	D55	A: increased affinity[33]	D52	
	2.60	L65	F: no variation [32]	F62	
TM3	3.25	C80	A/S: no detectable binding [35]	C77	
	3.27	M82	F: no variation [35]	F79	
	3.30	C85	A/S: reduced 4- to 13-fold [35]	C82	
	3.31	P86	F: reduction of affinity [32]	F83	
	3.32	V87	A: no variation [32]	V84	L: marginal variation [36]
	3.33	L88	A: reduction of affinity [32] [a]	L85	
	3.36	T91	A: reduction of affinity [32]	T88	A: reduction of affinity [37]
	3.37	Q92	A: reduction of affinity [32]	Q89	A: increased affinity [37]
	3.38	S93	A: no variation [33]	S90	A: marginal variation [38]
	3.39	S94	A: no detectable binding [33]	S91	A: marginal variation [37]
TM4	4.49	C131	A: no variation [38]	C128	
	4.53	S135	A: no variation [38]	S132	
	4.59	T141	A: no variation [38]	T138	
	4.62	F144	L: no variation [38]	L141	
L 4–5		R154		E151	A: loss of affinity [27]
		C169	A: no detectable binding [35]	C166	
		E172		E169	A: loss of affinity [27]
		K173		D170	K: no variation [27]
		S176		P173	R: no variation [27]
TM5	5.41	F184		F180	A: marginal variation [40]
	5.42	N185		N181	S: reduction of affinity [40]
	5.43	F186		F182	A: loss of affinity [40]
TM6	6.52	H251	A: no variation [39]	H250	L: loss of affinity [39]
	6.55	N254		N253	A: loss of affinity [40]
	6.56	C255	A: no variation [35]	C254	A: marginal variation [40]
	6.59	L258		F257	A: loss of affinity [40]
L 6–7		C260	A: no variation [35]	C259	
		C263	A: no variation [35]	C262	G: no variation [35]
TM7	7.39	I274		I274	A: loss of affinity [40]
	7.42	T277	A: reduction of affinity [41]	S277	A: reduction of affinity [40]
	7.43	H278	L: loss of affinity [42]	H278	A: loss of affinity [40]
	7.46	S281		S281	A: loss of affinity [40]

stants; moreover also the main ligand–receptor interactions (shown in Table 2) were restrained. More specifically, an initial restraint with a force constant of 10 kcal mol^{-1} $Å^{-2}$ was applied on all the alpha carbons, this force constant decreased during the whole MD, and in the last 200 ps, its value was 0.1 kcal mol^{-1} $Å^{-2}$. As regards the intra-helix H bonds and the main ligand–receptor interactions, a restraint of 10 and 50 kcal mol^{-1} $Å^{-2}$ was applied.

Every 200 ps of MD simulation, the conformation with respect to which the alpha-carbon restraints were defined was updated; this fact, together with the intra-helix H bond constraints, allowed us to take into account the effects of the non-conserved prolines on the helix conformation.

After the MD, three steps of minimisation were applied to the structure obtained as the average of the last 100 ps. During all these steps, a restraint of 0.1 kcal mol^{-1} $Å^{-2}$ was applied to the alpha carbons, and the restraint on the intra-helix H bonds was removed, while as regards the main ligand–receptor interaction in the first two steps, a restraint of 30 and 10 kcal mol^{-1} $Å^{-2}$ was applied, respectively, and in the last step the restraint was removed.

The same procedure was applied to several different starting interaction geometries, with the aim of exploring other binding possibilities, but at the end of the modelling procedure, only the above-described one shown in Fig. 2a maintained all the interactions considered important by mutagenesis studies (see Table 1).

With the aim of validating this model, 300 ps of MD simulation were performed, in which the backbone of the receptor was fixed, but all the ligand–receptor restraints were removed; a sampling of the last 200 ps conformation showed that during the simulation, none of the main ligand–receptor interactions were missed (the variation of the interatomic distances corresponding to these interactions was always less than 20%). Furthermore, the average of the last 200 ps was minimised without constraints, and the superimposition between the initial and the final CPA conformation showed an RMSD of 0.96 Å.

Table 2
Ligands used to perform the docking and their main interactions with the two receptors

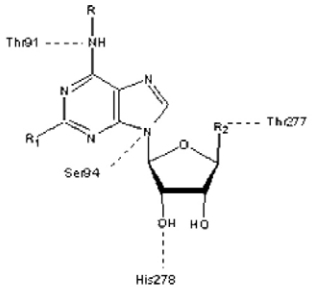

	R	R1	R2
CPA	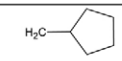	H	CH_2-OH
RPIA	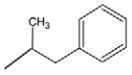	H	CH_2-OH
CADO	H	Cl	CH_2-OH
NECA	H	H	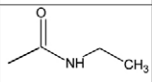
CGS21680 [a]	H	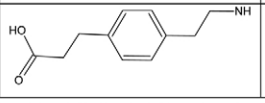	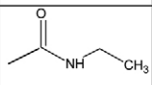

[a]CGS21680 presents a further interaction at the level of the carboxylic group with Asn181

The backbone conformation was also evaluated by inspection of the Psi/Phi Ramachandran plot obtained from PROCHECK analysis [43].

As shown in the Ramachandran plot in Fig. 3, the distribution of the Psi/Phi angles of the model is within the allowed regions and no residues have disallowed conformations.

In order to obtain the A_{2a}AR model we applied the same procedure described above, using two starting structures as templates: bovine rhodopsin and the A_1AR model obtained after the first 200 ps of MD. As the two results differ very slightly, we preferred to use the second model, because in this way, the manual rotation of the TM3 was identical in both receptors.

The obtained A_{2a}AR model was complexed with a high affinity ligand, and the complex was optimised. The complex modelling was carried out by using CGS-21680 [8], a selective agonist, considering the interactions with N6.55(253), S7.42 (277), H7.43(278) and S7.46(281), suggested by mutagenesis data (see Table 1).

Also for CGS-21680 some other starting binding positions were considered but, like CPA with the A_1AR, at the end of the modelling procedure, none of them maintained all the interactions considered important by mutagenesis data.

At this point the docking of the A_1AR selective agonists CPA, RPIA, CADO, the non-selective agonist NECA and the A_{2a}AR selective agonists CGS-21680 was performed manually in both receptors. All the compounds tested present the adenine group as their central core, and the initial docking position of the ligands was obtained by superimposing this group on those of the final structure of CPA and CGS-21680 in the A_1 and A_{2a}AR, respectively. In this position, all ligands exhibit the interaction suggested by mutagenesis data (see Table 2).

The ligand geometry was optimised at the AM1 level, and the atomic charges were calculated using the RESP [31] method with the 6-31G* wave function. To model the various ligand–receptor complexes, 800 ps of molecular dynamics were applied in the same conditions described above, using a constraint scheme analogous to the one used for A_1 and A_{2a}AR complex modelling.

3. Results and discussion

In general, docking of agonists to GPC receptors is subject to greater uncertainty than antagonists, as rhodopsin is crystallised in its inactive state. Until now, there is only a rough picture of the conformational changes that occur during receptor activation. Recent studies suggest that receptor activation could be due to a different rearrangement of TM3 and TM6 [44]. Furthermore, on the basis of UV absorption analysis, it has been suggested that when rhodopsin is activated, the χ1 rotamer of the high conserved residue W6.48(265) shifts from gauche+ to trans [45]; and recently, a 3D model for meta-II rhodopsin was published, featuring a similar change to the conformation of W6.48 [46].

Interestingly, this rotamer switch was also confirmed in the present study: during the MD simulation of both the A_1 and the A_{2a}AR complexed with all the agonists, the χ1 rotamer of W6.48 spontaneously shifted from gauche+ to trans. Therefore, for our purposes, although we do not wish to neglect other dynamic features of the GPCR structure, we prefer, in the absence of a crystal structure of a representative activated GPCR, not to change the template on the basis of hypothesised structures that may turn out to be inaccurate.

Table 3 shows the residues involved in the first and second spheres of the binding sites for the ligand–receptor A_1 and A_{2a} complexes studied. For both receptors, the binding site is positioned between TM3, TM6 and TM7, and all the residues considered important by mutagenesis studies are in the first sphere of the binding site.

Table 4 shows the principal interactions of the different compounds inside the two receptors.

Fig. 2a shows the docking, in the A_1 and A_{2a}AR binding sites, of CPA, the most A_1AR selective ligand among those tested. In the A_1 subtype, according to the mutagenesis data, CPA gives H bonds with T3.36(91), S3.39(94), T7.42(277), H7.43(278) and lipophilic interactions with L3.33(88) (through the cyclopentyl moiety) and with F5.43(186), F6.44(243), W6.48(247) and L6.51(250) (through the adenosinic group). In the A_{2a} subtype, the H bonds are maintained, but the lipophilic interactions with L3.33(85), F6.44(242), W6.48(246) and L6.51(249) are absent, because of the different position assumed by CPA in this receptor.

The other two A_1AR selective agonists, RPIA and CADO, interact with both receptors in the same manner as CPA. They

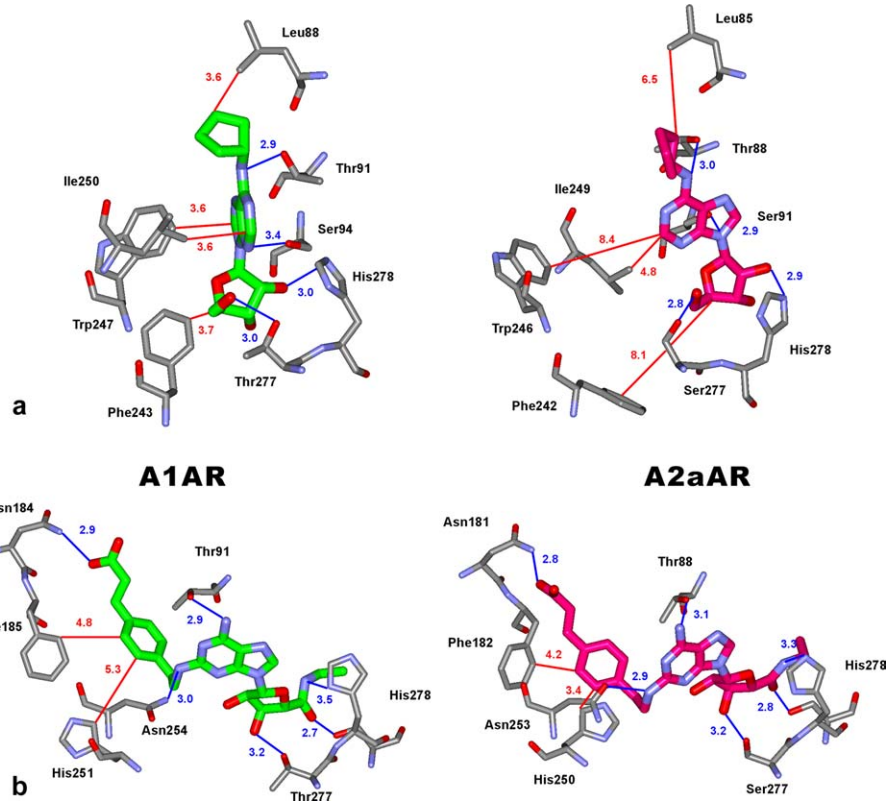

Fig. 2. **a.** CPA docked into the A_1AR (left) and A_{2a}AR (right) binding sites. **b.** CGS-21680 docked into the A_1AR (left) and A_{2a}AR (right) binding sites. Interatomic distances between H-bonded atoms are indicated in blue; carbon–carbon distances showing lipophilic interactions are indicated in red. All distances are in Angstroms.

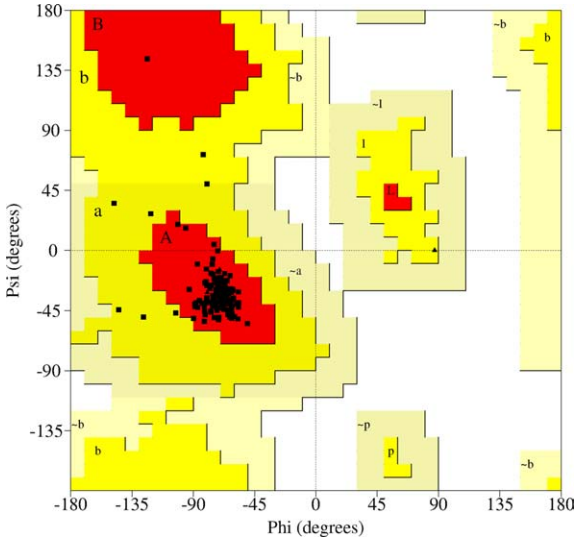

Fig. 3. Ramachandran plot of the A_1AR. The most favoured regions are coloured red, additional allowed, generously allowed and disallowed regions are indicated as yellow, light yellow and white fields, respectively.

Table 3
Residues involved in binding sites of A_1 and A_{2a} receptors. Residues in the first sphere are involved in the binding site with a distance lower than 4 Å, the second sphere includes the residues involved in the binding site with a distance between 4 and 6 Å. Residues that appear from mutagenesis to be of crucial importance are indicated in bold, while non-conserved residues are highlighted in grey

Receptor	Residues first sphere	Residues second sphere
A_1AR	**L3.33(88)**, L3.35(90), **T3.36 (91)**, **Q3.37(92)**, **S3.39(94)**, I3.40(95), A3.42(97), L3.43 (98), F5.43(186), F6.44(243), S6.47(246), W6.48(247), L6.51 (250), N6.55(254), I7.39(274), **T7.42(277)**, **H7.43(278)**, S7.46 (281)	L2.46(51), V3.32(87), V4.56 (138), G4.57(139), V5.39(182), Y5.40(183), N5.42(185), W5.46 (189), V5.47(190), H6.52(251), L6.59(258), A7.47(282)
A_{2a}AR	A2.49(51), V2.53(55), V3.32 (84), L3.35(87), **T3.36(88)**, S3.39(91), V5.39(178), **N5.42 (181)**, **F5.43(182)**, L6.51(249), **H6.52(250)**, **N6.55(253)**, **F6.59 (257)**, **I7.39(274)**, **S7.42(277)**, **H7.43(278)**, **S7.46(281)**	L2.46(48), D2.50(52), L3.33 (85), Q3.37(89), I3.40(92), L3.43(95), P4.60(139), W6.48 (246), I6.54(252), C6.56(254), T6.58(256), M7.35(270), N7.45 (280)

present in both receptors the H bonds with T3.36, S3.39, T7.42, and H7.43 and show only in the A_1 subtype lipophilic interactions with F5.43(186), F6.44(243), W6.48(247). NECA, instead, which has a similar activity in the two receptors, possesses, besides the H bonds showed by the other ligands, a further H bond in the A_{2a}AR with N6.55(253), which is suggested by mutagenesis studies to be of great importance for this receptor subtype. Furthermore, this agonist shows a lipophilic interaction with L6.51 and F6.44 in both the A_1AR and the A_{2a}AR.

Fig. 2b illustrates CGS-21680 docked into both sites of the A_1AR (on the left) and the A_{2a}AR (on the right); it also shows

Table 4
Principal interactions between the ligands and the binding site residues of the two receptors. The distances (Å) of hydrogen bond (HB) and lipophilic (LIPO) interactions are reported together with the group of the ligand giving the interaction (Aden = adenine ring; NH = N substituent of the adenine ring; R[X] = X group of the R substituent; see Table 3). Distances greater than 5 Å for HB and 7 Å for LIPO were not considered

Residues	CPA		CADO		RPIA		NECA		CGS-21680	
HB	A_1AR	A_{2a}AR	A_1AR	A_{2a}AR	A_1AR	A_{2a}AR	A_1AR	A_{2a}AR	A_1AR	A_{2a}AR
T3.36	NH 2.94	NH 3.00	NH_2 2.93	NH_2 2.95	NH 3.29	NH 3.03	NH_2 3.38	NH_2 2.87	NH_2 2.93	NH_2 3.07
S3.39	Ribose 2.83	Aden 2.90	Aden 3.10	Aden 2.90	Aden 3.33	Ribose 2.85	Ribose 2.95	Aden 2.93	R[NH] 2.93	Ribose 3.52
N5.42	–	–	–	–	–	–	–	–	R_1[COO]2.9	R_1[COO]2.8
N6.55	–	Aden 4.14	–	Aden 4.06	–	NH 4.08	–	NH_2 3.13	R_1[NH] 3.04	R_1[CO] 2.93
T/S7.42	R_2[OH] 3.03	R_2[OH] 2.79	R_2[OH] 2.84	R_2[OH] 2.86	R_2[OH] 2.78	R_2[OH] 2.85	R_2[CO] 2.80	R_2[CO] 2.82	Ribose 3.22	Ribose 3.16
H7.43	Ribose 3.04	Ribose 2.86	Ribose 2.89	Ribose 3.05	Ribose 3.04	Ribose 3.01	Ribose 3.05	Ribose 3.09	Ribose 2.95	Ribose 3.26
S7.46	Ribose 3.37	Ribose 4.03	–	–	Ribose 4.10	R_2[OH] 3.78	Ribose 4.09	R_2[NH] 3.38	R_2[CO] 2.74	R_2CO 2.77
LIPO										
L3.33	R[cicle] 3.58	R[cicle] 6.48	–	–	R[Phe] 4.20	R[Phe] 6.06	–	–	–	R_1[Phe] 4.55
F5.43	R[cicle] 5.59	–	Aden 5.17	–	R[Phe] 3.97	–	Aden 6.74	–	R_1[Phe] 4.84	R_1[Phe] 4.23
F6.44	Ribose 3.64	–	Aden 3.12	–	Ribose 3.73	–	Aden 4.81	R_2[CH_3] 3.87	Ribose 4.19	–
W6.48	Aden 3.89	–	Aden 3.35	–	Aden 3.71	–	–	–	R_1[Phe] 4.84	R_1[Phe] 6.90
L6.51	Aden 3.57	Aden 4.49	Aden 4.36	Aden 4.43	Aden 3.60	Aden 5.16	Aden 4.54	Aden 3.98	Ribose 4.27	Aden 5.70
H6.52	–	Aden 6.33	–	Aden 6.20	–	–	–	Aden 6.45	R_1[Phe] 5.72	R_1[Phe] 3.40
L/F6.59	R[cicle] 6.04	R[cicle] 5.83	–	–	R[Phe] 3.89	R[CH_3] 4.04	–	–	R_1[Phe] 5.08	R_1[CH_2]3.95
I7.39	Aden 4.86	Aden 5.24	Ribose 4.68	Ribose 5.63	Ribose 5.09	Ribose 4.57	Aden 4.34	Ribose 5.21	Aden 3.75	Aden 4.31

that the ligand interacts with T3.36, N5.42, N6.55, S7.42, H7.43 and S7.46 through H bonds. In the A_{2a}AR, the aromatic substituent is stabilised by F5.43(182) and H6.52(250) residues (at 4.2 and 3.4 Å from the aromatic ring), whereas in the A_1AR, these residues are far away (4.8 and 5.7 Å from the aromatic ring), and are unable to interact with CGS-21680.

Fig. 4a shows the volumes of the cavities between CPA and the two ARs, thus indicating the different dimensions of the two binding sites, which could be important in determining the selectivity of the derivatives considered.

The A_1AR binding site cavity is small and allows close interaction with the ligand, while in the A_{2a}AR , less bulky ligands like CPA cannot occupy the larger site so efficiently.

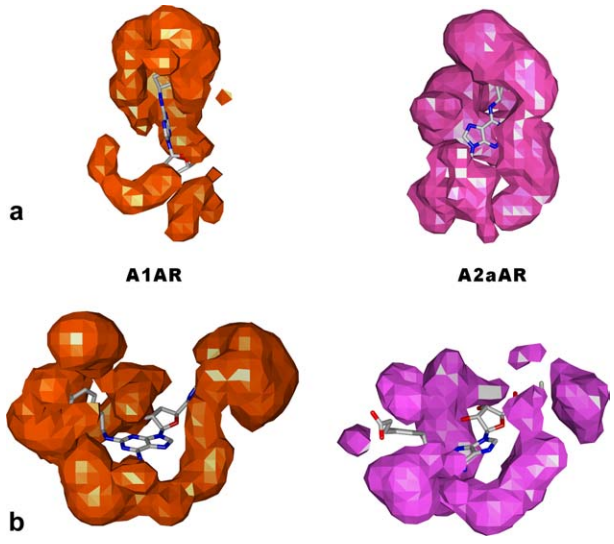

Fig. 4. **a.** CPA docked into the A_1AR (left) and A_{2a}AR (right) binding sites. The volumes of the cavities between CPA and the two receptors are shown. **b.** CGS-21680 docked into the A_1AR (left) and A_{2a}AR (right) binding sites. The volumes of the cavities between CGS-21680 and the two receptors are shown.

As regards the binding of CGS-21680, Fig. 4b confirms that in the A_{2a}AR, the aromatic substituent is effectively stabilised, whereas in the A_1AR, the large dimensions of the pocket where the substituent is inserted do not allow a strong interaction.

All these observations are confirmed by the energy calculations of the ligand–receptor interactions obtained by means of the Batchmin programme [20] on the final structures of the complexes (see Table 5).

The interaction energies between the receptor and the ligand were calculated by subtracting the energy of the separate ligand and receptor from the energy of the receptor–ligand complex. These energies are not rigorous thermodynamic quantities, but can only be used to compare the relative stability of the complexes of the same ligand in different receptors. Consequently, these interaction energy values cannot be used to predict binding affinities, since changes in entropy and solvation effects are not taken into account.

These calculations underline the fact that A_1/A_{2a} selectivity is mainly influenced by the different ability of the two receptors to give lipophilic interactions, instead of giving different H bonds. This would confirm the hypothesis that A_1AR-selective ligands exhibit a lower level of interaction in the A_{2a}AR due to the larger dimensions of the binding site cavity, which does not allow a strong lipophilic interaction. Analogously, in the case of CGS-21680, the low activity shown in the A_1AR could be due to the low stabilisation of the aromatic substituent inside the lipophilic pocket.

As shown in Table 3, there are only few non-conserved residues among the A_1 and A_{2a} binding sites, and they cannot justify the different binding cavity size. However, on comparing the two receptors, we observe a different disposition of the TMs: this could be due to the fact that in the A_1AR, the residues P1.48(25), P3.31(86) and P5.49(192) act as flexible mo-

Table 5
Binding affinity (K_i values with 95% confidence intervals or ± S.E.M. in parentheses) and interaction energy (kcal/mol) of selective agonists for the A_1AR and the A_{2a}AR [38]. Total indicates the sum of the Van der Walls (VdW) and electrostatic (Elect) terms

Ligand	A_1 receptor				A_{2a} receptor			
	K_i (nM)	Interaction energy (kcal/mol)			K_i (nM)	Interaction energy (kcal/mol)		
		VdW	Elect.	Total		VdW	Elect.	Total
CPA	2.3 (1.5–3.4)	–29.10	–2.65	–31.75	790 (470–1360)	–22.63	–4.12	–26.76
CADO	1.39 (1.28–1.51)	–28.45	–3.59	–32.04	180 (150–220)	–20.38	–3.44	–23.82
RPIA	2.0 (1–4.2)	–31.66	–2.45	–34.11	860 (480–1540)	–29.50	–2.51	–32.01
NECA	14 (6.4–29)	–23.45	–2.72	–26.17	20 (12–35)	–25.33	–2.56	–27.90
CGS-21680	290 (230–360)	–43.10	–6.93	–50.03	27 (12–59)	–46.48	–7.16	–53.64

Table 6
Inter-helix H-bonds in the $A_1$and A_{2a}AR found after molecular modelling optimisation

Inter-helix bonds in the A_1 receptor	Inter-helix bonds in the A_{2a} receptor
S2.45(50)-W4.50(132)	E1.39(13)-Y7.36(271)
I3.34(89)-S4.53(135)	F2.42(47)-A3.45(97)
I3.46(101)-Y7.53(288)	Q3.37(89)-N5.42(181)
Y5.40(183)- H6.52(251)	A3.47(99)-Y5.58(197)
Y5.58(201)-L6.41(240)	
I6.40(239)-N7.45(280)	

The S2.45(50)-W4.50(132) H bond is lacking in the CADO and CGS21680-A_1AR complex, while the A3.47(99)-Y5.58(197) in the CGS21680-A_{2a}AR complex is replaced by Y5.58(197)-V6.41(39).

lecular hinges, changing the folding of the helices of TM1, TM3 and TM5; in the A_{2a}AR, these residues are not conserved, thus determining a different rearrangement of the helices, with the formation of a large binding site cavity. Site-directed mutagenesis shows that in the A_1 receptor, the substitution of the P1.48(25) and P3.31(86) with leucine and phenylalanine, respectively, causes a reduction in agonist affinity (see Table 1), suggesting their structural role.

The different disposition of the helices is confirmed by an analysis of the H bonds that spontaneously form during the MD of the complexes and are present at the end of the modelling procedure in all the ligand–receptor complexes (see Table 6). This rearrangement in the A_{2a}AR concerns only TM2, TM3 and TM5, leaving the binding site free.

In the A_1AR, instead, H bonds are generated, involving and re-arranging all the TM domains, and turning the side chains into the inter-helix space. In particular the interactions of L6.41 (240) with Y5.58(201) and of H6.52(251) with Y5.40(183), drag F6.44(243), W6.48(247) and L6.51(250) towards the binding cavity, allowing an effective stabilisation of the adenosinic group of the agonists.

4. Conclusions

We have provided 3D models of the A_1 and A_{2a} adenosine receptors, based on the highest resolution structure of bovine rhodopsin. A model of the agonist–receptor complexes was constructed and validated by means of docking studies. The structural effects of ligand binding have been examined on the basis of hydrogen bonds, lipophilic interactions and binding energies in the final complexes obtained from manual docking. Results show that A_1/A_{2a} selectivity is not mainly influenced by a different H bond network between ligand and receptor, as the selective A_1 agonists present the same H interactions in both receptors. What appears to be decisive is the lipophilic factor: in the A_1 subtype, the compounds with a high affinity present lipophilic interactions with L3.33(88), F5.43 (186), F6.44(243), W6.48(247) and L6.51(250). Among them, the only residue that has been tested by mutagenesis in the A_1AR is L3.33(88). In our model, this amino acid shows a strong interaction with the N^6-substituted ligands (CPA and RPIA), and this is in agreement with the mutagenesis studies that highlight an important interaction with these compounds [32].

As regards the A_{2a} affinity, our studies have confirmed that the interaction with N6.55(253) is crucial, moreover, the docking of CGS21680 shows that the selectivity of this compound could be due to the presence of the R1 substituent, which is able to interact with the lipophilic residues of TM5 and TM6.

The different lipophilic interaction in the two receptors seems to be mediated by the different dimensions of the inter-helix channel, due to the structural diversity of the two re-

ceptors and to the consequent diversity of the inter-helix H-bond network. In particular, three non-conserved prolines, P1.48(25), P3.31(86) and P5.49(192), allow a different interaction in the A_1 receptor between the TMs, thus determining a smaller binding site cavity. These differences allow ligands with large substituents, like CGS-21680, to interact well with the A_{2a}AR; in the A_1AR, instead, the small dimensions of the binding site allows a good interaction only with small ligands, like adenosine.

Acknowledgments

This work was supported by MIUR and University of Pisa.

References

[1] B.B. Fredholm, M.P. Abbracchio, G. Burnstock, G.R. Dubyak, T. K. Harden, K.A. Jacobson, U. Schwabe, M. Williams, Trends Pharmacol. Sci. 18 (1997) 79–82.
[2] F. Libert, S.N. Schiffmann, A. Lefort, M. Parmentier, C. Gerard, J. E. Dumont, J.J. Vanderhaeghen, G. Vassart, EMBO J. 10 (1991) 1677–1682.
[3] F. Libert, J. Van Sande, A. Lefort, A. Czernilofsky, J.E. Dumont, G. Vassart, H.A. Ensinger, K.D. Mendla, Biochem. Biophys. Res. Commun. 187 (1992) 919–926.
[4] A. Townsend-Nicholson, J. Shine, Brain Res. Mol. Brain Res. 16 (1992) 365–370.
[5] V. Ralevic, G. Burnstock, Pharmacol. Rev. 50 (1998) 413–492.
[6] J.S. Fink, D.R. Weaver, S.A. Rivkees, R.A. Peterfreund, A.E. Pollack, E. M. Adler, S.M. Reppert, Brain Res. Mol. Brain Res. 14 (1992) 186–195.
[7] R.F. Bruns, Ann. N. Y. Acad. Sci. 603 (1990) 211–225.
[8] M.F. Jarvis, R. Schulz, A.J. Hutchison, U.H. Do, M.A. Sills, M. Williams, J. Pharmacol. Exp. Ther. 251 (1989) 888–893.
[9] I. Feoktistov, R. Polosa, S.T. Holgate, I. Biaggioni, Trends Pharmacol. Sci. 19 (1998) 148–153.
[10] C.E. Müller, B. Stein, Curr. Pharm. Des. 2 (1996) 501–530.
[11] S.-A. Poulsen, R.J. Quinn, Bioorg. Med. Chem. 6 (1998) 619–641.
[12] C.E. Muller, Expert Opin. Ther. Pat. 7 (1997) 419–440.
[13] S. Hess, Expert Opin. Ther. Pat. 11 (2001) 1533–1561.
[14] T.W. Stone, M.G. Collis, M. Williams, L.P. Miller, A. Karasawa, D. Hillaire-Buys, In Pharmacological Sciences: Perspectives for Research and Therapy in the Late 1990s.
[15] A.C. Cuello, B. Collier (Eds.), Birkhauser Verlag, Basel, Switzerland, 1995, pp. 303–309.
[16] P.J. Richardson, H. Kase, P.G. Jenner, Trends Pharmacol. Sci. 18 (1997) 338–344.
[17] C. Ledent, J.M. Vaugeois, S.N. Schiffmann, T. Pedrazzini, M. El Yacoubi, J.J. Vanderhaeghen, J. Costentin, J.K. Heath, G. Vassart, M. Parmentier, Nature 388 (1997) 674–678.
[18] P.G. Baraldi, B. Cacciari, G. Spalluto, A. Borioni, M. Viziano, S. Dionisotti, E. Ongini, Curr. Med. Chem. 2 (1995) 707–722.
[19] K. Palczewski, T. Kumasaka, T. Hori, C.A. Behnke, H. Motoshima, B. A. Fox, I. Le Trong, D.C. Teller, T. Okada, R.E. Stenkamp, M. Yamamoto, M. Miyano, Science 289 (2000) 739–745.
[20] Macromodel ver. 7.0, Schrodinger Inc., 1999.
[21] WebLab Viewer Pro 3.7 (Accelrys Inc., San Diego, CA).
[22] E.F. Pettersen, T.D. Goddard, C.C. Huang, G.S. Couch, D.M. Greenblatt, E.C. Meng, T.E. Ferrin, J. Comput. Chem. 25 (2004) 1605–1612.
[23] Gaussian 98, a.5. M.J. Frisch, G.W. Trucks, H.B. Schlegel, G.E. Scuseria, M.A. Robb, J.R. Cheeseman, V.G. Zakrzewski, J.A. Montgomery, R. E. Stratmann, J.C. Burant, S. Dapprich, J.M. Millam, A.D. Daniels, K.N. Kudin, M.C. Strain, O. Farkas, J. Tomasi, V. Barone, M. Cossi, R. Cammi, B. Mennucci, C. Pomelli, C. Adamo, S. Clifford, J. Ochterski, G.A. Petersson, P.Y. Ayala, Q. Cui, K. Morokuma, D.K. Malick, A.D. Rabuck, K. Raghavachari, J.B. Foresman, J. Cioslowski, J.V. Ortiz, B.B. Stefanov, G. Liu, A. Liashenko, P. Piskorz, I. Komaromi, R. Gomperts, R.L. Martin, D.J. Fox, T. Keith, M.A. Al-Laham, C.Y. Peng, A. Nanayakkara, C. Gonzalez, M. Challacombe, P.M.W. Gill, B.G. Johnson, W. Chen, M.W. Wong, J.L. Andres, M. Head-Gordon, E.S. Replogle, J. A. Pople, Gaussian, Inc., Pittsburgh PA, 1998.
[24] J.A. Ballesteros, H.W. Weinstein, Methods in Neurosci. 25 (1995) 366–428.
[25] GPCRDB, Information system for G protein-coupled receptors (GPCRs), www.gpcr.org.
[26] M.E. Olah, K.A. Jacobson, G.L. Stiles, J. Biol. Chem. 269 (1994) 24692–24698.
[27] J. Kim, Q. Jiang, M. Glashofer, S. Yehle, J. Wess, K.A. Jacobson, Mol. Pharm. 49 (1996) 683–691.
[28] A. Scott, M.E. Rivkees, H. Lasbury, Barbhaiya, J. Biol. Chem. 270 (1995) 20485–20490.
[29] J.D. Thompson, D.G. Higgins, T.J. Gibson, Nucleic Acids Res. 22 (1994) 4673–4680.
[30] R. Fredriksson, M.C. Lagerström, L.G. Lundin, H.B. Schiöth, Mol. Pharm. 63 (2003) 1256–1272.
[31] C.I. Bayly, P. Cieplak, W.D. Cornell, P.A. Kollman, J. Phys. Chem. 97 (1993) 10269–10280.
[32] S.A. Rivkees, H. Barbhaiya, A.P. IJzerman, J. Biol. Chem. 274 (1999) 3617–3621.
[33] H. Barbhaiya, R. McClain, A. Ijzerman, S.A. Rivkees, Mol. Pharmacol. 50 (1996) 1635–1642.
[34] Z. Gao, Q. Jiang, K.A. Jacobson, A.P. Ijzerman, Biochem. Pharmacol. 60 (2000) 661–668.
[35] D.J. Scholl, J.N. Wells, Bioc. Pharm. 60 (2000) 1647–1654.
[36] Q. Jiang, B.X. Lee, M. Glashofer, A.M. van Rhee, K.A. Jacobson, J. Med. Chem. 40 (1997) 2588–2595.
[37] Q. Jiang, A.M. Van Rhee, J. Kim, S. Yehle, J. Wess, K.A. Jacobson, Mol. Pharmacol. 50 (1996) 512–521.
[38] B.B. Fredholm, A.P. IJzerman, K.A. Jacobson, K.N. Klotz, J. Linden, Pharm. Rev. 53 (2001) 527–552.
[39] Z.G. Gao, A. Chen, D. Barak, S.K. Kim, C.E. Müller, K.A. Jacobson, J. Biol. Chem. 277 (2002) 19056–19063.
[40] J. Kim, J. Wess, A.M. van Rhee, T. Schoneberg, K.A. Jacobson, J. Biol. Chem. 270 (1995) 13987–13997.
[41] M.E. Olah, G.L. Stiles, Pharm. Ther. 85 (2000) 55–75.
[42] E.S. Dawson, J.N. Wells, Mol. Pharm. 59 (2001) 1187–1195.
[43] R.A. Laskowski, M.W. MacArthur, D.S. Moss, J.M. Thorton, J. Appl. Crystallogr. 26 (1993) 283–291.
[44] J.A. Ballesteros, A.D. Jensen, G. Liapakis, S.G.F. Rasmussen, L. Shi, U. Gether, J.A. Javitch, J. Biol. Chem. 276 (2001) 29171–29177.
[45] R. Croce, J. Breton, R. Bassi, Biochem. 35 (1996) 11149–11159.
[46] G.V. Nikiforovich, G.R. Marshall, Biochem. 42 (2003) 9110–9120.